Nuclear Physics **A440** (1985) 274–300

CALCULATED ISOSPIN-MIXING CORRECTIONS TO FERMI β-DECAYS IN 1s0d-SHELL NUCLEI WITH EMPHASIS ON $A = 34$

W. E. ORMAND and B. A. BROWN

National Superconducting Cyclotron Laboratory, Michigan State University, East Lansing, Michigan 48824, USA

Received 2 January 1985

Abstract: Corrections to the Fermi matrix element due to analogue symmetry breaking are evaluated for the superallowed β-decays of ^{22}Mg, ^{34}Cl, and ^{34}Ar by considering the effects of Coulomb and other isospin-nonconserving potentials. Analogue symmetry breaking is calculated within the shell-model formalism by considering: (i) the deviations from unity of the radial overlap between the proton and neutron single-particle wave functions, and (ii) isospin mixing between states within the $0d_{5/2}0d_{3/2}1s_{1/2}$ shell. The radial-overlap corrections for several cases of interest in the sd shell are evaluated with single-particle wave functions obtained from a self-consistent Hartree-Fock calculation. The sd-shell isospin-mixing corrections are calculated with an isospin-non-conserving potential which reproduces the experimental isobaric mass shifts. Comparisons with previous calculations are made. The Fermi matrix elements for the isospin-forbidden β-decays of ^{34}Cl and ^{34}Ar to excited 0^+ states are also calculated.

1. Introduction

Superallowed Fermi β-transitions between $J^\pi = 0^+$, $T = 1$ analogue states have been the subject of much study [1–8]) and some controversy [9, 10]) over the past years. An important feature of these transitions is that since they are purely vector it is possible to extract from their ft values an accurate determination of the effective vector coupling constant for single-nucleon β-decay, provided that nuclear structure corrections to the Fermi matrix element can be properly accounted for. This is important because the difference between this effective vector coupling constant and the coupling constant for the muon decay is dependent on radiative correctons to both decays and the Cabibbo angle. By determining these coupling constants from experimental data it is possible to test current theories for the radiative corrections and deduce empirical values for the fundamental vector coupling constant and the Cabibbo angle.

For Fermi transitions the relationship between the half-life, vector coupling constant, and the Fermi matrix element is

$$f_R t = \frac{K}{G_V^2 |M_F|^2}, \tag{1.1}$$

where

$$K = \frac{2\pi^3 \ln 2 \hbar^7 c^6}{(mc^2)^5}.$$

The quantities in this equation are the statistical rate function f, the partial half-life t, the effective vector coupling constant for single-nucleon β-decay G_V, and the Fermi matrix element for the transition M_F. The statistical rate function is evaluated by solving the Dirac equation for the lepton in the static Coulomb potential of the residual nucleus, and is corrected with the nucleus dependent "outer" radiative correction δ_R of Sirlin [11]), i.e. $f_R = f(1+\delta_R)$. The effective coupling constant G_V includes the "inner" radiative correction Δ_β of ref. [11]) and is related to the fundamental coupling constant G_{V0} by

$$G_V^2 = G_{V0}^2 \cos^2\theta_C (1+\Delta_\beta)$$

where θ_C is the Cabibbo angle.

If the initial and final nuclear states are perfect analogues, then the Fermi matrix element is model independent and given by

$$M_{F0}^2 = [T(T+1) - T_{Zi}T_{zf}]\delta_{if}. \tag{1.2}$$

Values for G_V could then be extracted from measured ft values with eq. (1.1). The most accurately determined ft values, however, are not constant within experimental uncertainty as eq. (1.1) would indicate [12]). This suggests the possibility of the breaking of analogue symmetry between the initial and final nuclei due to the presence of isospin-nonconserving (INC) interactions. The theoretical evaluation of the deviation from analogue symmetry is still uncertain and has been a source of controversy [9, 10]) in the past.

In the present work we reexamine the correction to the Fermi matrix element in the light of recent advances in our understanding of nuclear structure. Wave functions for sd-shell nuclei, and in particular the upper sd shell (A = 28–39), have been improved with the development of the universal sd-shell (USD) hamiltonian of Wildenthal [13]). In this mass region the most accurately measured superallowed transition is for the ^{34}Cl decay and we will thus concentrate on the A = 34 mass system in this work.

Our work closely follows that of Towner and Hardy [6–8, 10]). In particular, we consider the correction to the Fermi matrix element as a sum of two facors. The first arises from isospin mixing between states within the sd-shell model space, while the other can be considered as due to mixing which occurs between states within the model space with those outside the model space (sect. 2). The "outside" mixing is calculated by considering the deviation from unity in the overlap of the radial

wave functions in the initial and final nuclei. We improve upon previous calculations of this radial-overlap contribution by using self-consistent Hartree-Fock radial wave functions rather than the conventional Woods-Saxon parameterization. We find that it is important to consider the effect of the isovector potential induced by the difference in the proton and neutron densities (sect. 3). Calculations of the contribution due to isospin mixing within the sd shell are also improved upon by constraining the INC interaction to reproduce the isobaric mass shifts for states in the $A = 34$–39 mass region (sect. 4). Fermi matrix elements for the isospin-forbidden decays of ^{34}Ar and ^{34}Cl are presented in sect. 5. In sect. 6, corrections for superallowed β-decays are summarized and discussed, the value for G_V, determined from ^{34}Cl decay, is compared to that for muon decay and discussed in terms of the Cabibbo angle and the inner radiative corrections.

2. Corrections to the Fermi matrix element δ_C

The extent to which analogue symmetry is broken is embodied in a correction factor δ_C to the Fermi matrix element defined by

$$|M_F|^2 = |M_{F0}|^2(1-\delta_C), \tag{2.1}$$

where M_{F0} is the Fermi matrix element between states with analogue symmetry given by eq. (1.2). The starting point for the calculation of δ_C is the spherical shell-model wave functions which consist of the many-body Slater determinants obtained within the spherical single-particle basis $|\psi(nlj)\rangle = R_{nlj}(r)[Y^l \times s]^j$. The model space for the nuclei considered consists of restricting 16 of the nucleons to the closed $0s_{\frac{1}{2}}0p_{\frac{3}{2}}0p_{\frac{1}{2}}$ shell configuration, while the remaining $A-16$ nucleons are restricted to the three orbits $0d_{\frac{5}{2}}$, $1s_{\frac{1}{2}}$, and $0d_{\frac{3}{2}}$. Within this basis we need to consider the effects of isospin mixing due to the INC interaction between states within this model space as well as with those outside. Isospin mixing within the model space is calculated by adding the INC interaction onto the isospin-conserving sd-shell hamiltonian. Isospin mixing outside the sd shell is taken into account by allowing the proton single-particle radial wave functions to be pushed out relative to the neutron single-particle wave functions due to the Coulomb single-particle potential. These two effects can be factored [6]) to give

$$\delta_C = \delta_{IM} + \delta_{RO},$$

where δ_{IM} is the contribution due to isospin mixing within the sd shell, and δ_{RO} is the contribution due to the deviation from unity of the overlap between the proton and neutron radial wave functions.

The Fermi matrix element for $\beta^{\pm}$ decay between analogue states having

approximate isospin is given by

$$M_{\mathrm{F}} = \langle \Psi(\Gamma', T_z')|\tau_{\pm}|\Psi(\Gamma, T_z)\rangle, \tag{2.2}$$

where Γ represents all quantum numbers other than the z-projection of the isospin such as total angular momentum J. The isospin convention used here is $\tau_z|\mathrm{p}\rangle = |\mathrm{p}\rangle$. Within the formalism of the shell model, eq. (2.2) for positron decay can be written as

$$M_{\mathrm{F}} = \sum_j \mathrm{OBTD}(j_{\mathrm{n}}, j_{\mathrm{p}}; \Delta J = 0)(2j+1)^{\frac{1}{2}}\Omega_j\langle \mathrm{n}|\tau_-|\mathrm{p}\rangle, \tag{2.3}$$

where

$$\Omega_j = \int \mathrm{d}r r^2 R_{\mathrm{n}}(r)R_{\mathrm{p}}(r),$$

$$\langle \mathrm{n}|\tau_-|\mathrm{p}\rangle = 1.$$

(The analogous formulae for the electron decay are obtained by interchanging the n/p labels.) The general form of the one-body transition density matrix (OBTD) in eq. (2.3) is given in proton-neutron formalism by [19] †

$$\mathrm{OBTD}(j'\mu', j\mu; \Delta J) = \frac{1}{(2\Delta J+1)^{\frac{1}{2}}}\langle \Psi(\Gamma', T_z')\|[a^{\dagger}_{j'\mu'} \times \tilde{a}_{j\mu}]^{\Delta J}\|\Psi(\Gamma, T_z)\rangle, \tag{2.4}$$

where $a^{\dagger}_{j\mu}$ is the tensor operator that creates a nucleon with $\tau_z = 2\mu$ in the orbit j, and $\tilde{a}_{j\mu}$ is the tensor operator that destroys a nucleon in the orbit j. Here we freely interchange the values $\mu = \frac{1}{2}$ $(-\frac{1}{2})$ with the labels p (n). The double bar in the reduced matrix element in eq. (2.4) denotes a reduction in angular momentum space.

If the effects of the INC forces are neglected, then the value of the sum in eq. (2.3) is given by eq. (1.2). However, deviations from this value occur at two levels. First, the one-body transition density matrix is slightly changed because of isospin mixing, and second, the radial-overlap integral Ω_j differs from unity because the proton single-particle wave functions are pushed out relative to the neutron wave functions.

We denote the correction to the one-body transition density matrix by the quantity $\beta(j_{\mathrm{n}}, j_{\mathrm{p}}; \Delta J = 0)$ defined as

$$\beta(j_{\mathrm{n}}, j_{\mathrm{p}}; 0) = \mathrm{OBTD}^{\mathrm{T}}(j_{\mathrm{n}}, j_{\mathrm{p}}; 0) - \mathrm{OBTD}(j_{\mathrm{n}}, j_{\mathrm{p}}; 0), \tag{2.5}$$

† Note that in ref. [19]) the second and third lines of eq. (14.60) should be divided by $[(1+\delta_{\rho_1\delta_{\rho_2}})(1+\delta_{\rho_3\delta_{\rho_4}})]^{1/2}$.

where the superscript T denotes the one-body transition density matrix obtained when both the initial and final states possess good isospin.

The proton and neutron single-particle wave functions used to evaluate Ω_j are dependent on the selection of the single-particle potential parameters, such as the well depth. In order to specify the separation energies needed for the calculations of the radial wave functions we insert a complete set of states $|\Psi(\pi)\rangle$ of the $A-1$ nucleon system between the creation and annihilation operator of $\mathrm{OBTD}^{\mathrm{T}}(j_{\mathrm{n}}, J_{\mathrm{p}}; 0)$. The general one-body transition density matrix $\mathrm{OBTD}^{\mathrm{T}}(j'\mu', j\mu; \Delta J)$ is then

$$\mathrm{OBTD}^{\mathrm{T}}(j'\mu', j\mu; \Delta J) = \sum_{\pi} (-1)^{J_\Gamma + J_\pi + j + \Delta J} [(2J_\Gamma + 1)(2J_{\Gamma'} + 1)]^{\frac{1}{2}} \times \begin{Bmatrix} J_{\Gamma'} & J_\Gamma & \Delta J \\ j' & j & J_\pi \end{Bmatrix} [S(j'\mu'; \Gamma', \pi) S(j\mu; \Gamma, \pi)]^{\frac{1}{2}}. \tag{2.6}$$

The spectroscopic factor $S(j\mu; \Gamma, \pi)$ is given in terms of the matrix element of $a^{\dagger}_{j\mu}$, reduced in angular momentum space, by

$$S(j\mu; \Gamma, \pi) = \left| \frac{\langle \Psi(\Gamma, T_z) \| a^{\dagger}_{j\mu} \| \Psi(\pi) \rangle}{(2J_\Gamma + 1)^{\frac{1}{2}}} \right|^2.$$

The proton-neutron spectroscopic factor $S(j\mu; \Gamma, \pi)$ is related to the spectroscopic factor in isospin formalism by

$$S(j\mu; \Gamma, \pi) = C^2(\mu) S(j; \Gamma, \pi), \tag{2.7}$$

where

$$C(\mu) = (T_\pi T_{\pi z} \tfrac{1}{2}\mu | T_\Gamma T_{\Gamma z}).$$

$S(j; \Gamma, \pi)$ is given in terms of the matrix element of $a^{\dagger}_j$, reduced in angular momentum and isospin space, by

$$S(j; \Gamma, \pi) = \left| \frac{\langle \Psi(\Gamma) \| \| a^{\dagger}_j \| \| \Psi(\pi) \rangle}{[(2J_\Gamma + 1)(2T_\Gamma + 1)]^{\frac{1}{2}}} \right|^2.$$

The proton and neutron radial wave functions are then evaluated with the appropriate separation energy to the intermediate parent state $|\Psi(\pi)\rangle$, and the radial integral of these wave functions, $\Omega_{j,\pi}$, is weighted by the factor $\sqrt{[S(j; \Gamma', \pi) S(j; \Gamma, \pi)]}$.

Utilizing eqs. (2.5), (2.6) and (2.7), with $\Delta J = 0$, the Fermi matrix element can now be rewritten as

$$M_{\mathrm{F}} = \sum_j \mathrm{OBTD}^{\mathrm{T}}(j_{\mathrm{n}}, j_{\mathrm{p}}; 0)(2j+1)^{\frac{1}{2}} - \sum_j \beta(j_{\mathrm{n}}, j_{\mathrm{p}}; 0)(2j+1)^{\frac{1}{2}} - \sum_{j,\pi} C(\tfrac{1}{2}\tfrac{1}{2})C(-\tfrac{1}{2})(2J_\Gamma + 1)^{\frac{1}{2}} [S(j; \Gamma', \pi) S(j; \Gamma, \pi)]^{\frac{1}{2}} (1 - \Omega_{j,\pi}). \tag{2.8}$$

For superallowed decays eq. (2.8) gives

$$|M_{\mathrm{F}}|^2 = |M_{\mathrm{F0}}|^2(1-\delta_{\mathrm{C}}) = |M_{\mathrm{F0}}|^2(1-(\delta_{\mathrm{RO}}+\delta_{\mathrm{IM}})), \tag{2.9}$$

where δ_{RO} and δ_{IM} are given by

$$\delta_{\mathrm{RO}} = \frac{2}{M_{\mathrm{F0}}} \sum_{j,\pi} C(\tfrac{1}{2})C(-\tfrac{1}{2})(2J_f+1)^{\frac{1}{2}} \times [S(j;f,\pi)S(j;f,\pi)]^{\frac{1}{2}}(1-\Omega_{j,\pi}), \tag{2.10a}$$

$$\delta_{\mathrm{IM}} = \frac{2}{M_{\mathrm{F0}}} \sum_{j} \beta(j_{\mathrm{n}}, j_{\mathrm{p}}; 0)(2j+1)^{\frac{1}{2}}. \tag{2.10b}$$

3. Radial-overlap contribution to δ_{C}

Previously [6-8]), values for δ_{RO} have been calculated using proton and neutron radial wave functions obtained with a central Woods-Saxon plus Coulomb potential. This procedure overestimates the difference between the proton and neutron radial wave functions by neglecting an induced isovector interaction that arises from the difference between the proton and neutron densities. To take into account the effects of this induced interaction we have performed self-consistent Hartree-Fock calculations with a Skyrme-type interaction.

Hartree-Fock calculations using the Skyrme interaction lead to a set of spherical nonlocal differential equations with eigenfunctions $\psi_\alpha^{\mathrm{NL}}(r) = u_\alpha^{\mathrm{NL}}(r)/r$ and eigenvalues ε_α [refs. [14-16])]. The nonlocal eigenfunctions and eigenvalues can be obtained from the following equivalent set of differential equations, which involve a local energy-dependent potential [15]):

$$-\frac{\hbar^2}{2m}\frac{\mathrm{d}^2}{\mathrm{d}r^2}u^{\mathrm{L}}_{\alpha,\mu}(r) + \frac{\hbar^2}{2m}\frac{l(l+1)}{r^2}u^{\mathrm{L}}_{\alpha,\mu}(r) + V^{\mathrm{L}}_{\mu}(r)u^{\mathrm{L}}_{\alpha,\mu}(r) = \varepsilon_\alpha u^{\mathrm{L}}_{\alpha,\mu}(r) \tag{3.1}$$

with

$$V^{\mathrm{L}}_{\mu}(r) = [1-m^*(r)/m]\varepsilon_{\alpha,\mu} + U_\mu(r) + U^{\mathrm{SO}}_\mu(r)\boldsymbol{\sigma}\cdot\boldsymbol{l} + \delta_{\frac{1}{2},\mu}V_{\mathrm{Coul}}(r),$$

$$m^*(r)/m = \{1 + C_0[\rho_{\mathrm{p}}(r)+\rho_{\mathrm{n}}(r)] + 2\tau C_1[\rho_{\mathrm{p}}(r)+\rho_{\mathrm{n}}(r)]\}^{-1},$$

$$\psi^{\mathrm{NL}}_{\alpha,\mu}(r) = N[m^*(r)/m]^{\frac{1}{2}}\psi^{\mathrm{L}}_{\alpha,\mu}(r).$$

N is the normalizing constant determined by the condition

$$\int |\psi^{\mathrm{NL}}_{\alpha,\mu}(r)|^2 r^2 \mathrm{d}r = 1.$$

The subscript μ denotes the z-projection of the isospin of the nucleon, and α denotes all other single-particle quantum numbers.

The central $U_\mu(r)$ and spin-orbit $U_\mu^{SO}(r)$ potentials are functions dependent on the Skyrme parameters and the densities [16]. The coefficients C_0 and C_1 expressed in terms of the Skyrme parameters t_1 and t_2 are

$$C_0 = \frac{2m}{\hbar^2}\left[\frac{5t_2+3t_1}{16}\right],$$

$$C_1 = \frac{2m}{\hbar^2}\left[\frac{(t_2-t_1)}{16}\right].$$

The Coulomb potential V_{Coul} is

$$V_{\text{Coul}}(r) = e^2\left[\int\frac{\rho_p(r')}{|r'-r|}\,d^3r - \frac{3}{4}\left(\frac{3}{\pi}\right)^{\frac{1}{3}}\int\rho_p^{\frac{4}{3}}(r)\,d^3r\right],$$

where the first of the two contributions is the direct term, and the second the exchange term in the Fermi-gas approximation [16]. The nucleon densities $\rho_\mu(r)$ are given by

$$\rho_\mu(r) = \sum_j n_{j,\mu}|\psi^{NL}_{\alpha,\mu}(r)|^2,$$

where $n_{j,\mu}$ is the occupation number of the jth orbit as determined from the sd-shell-model wave functions.

First, the average central potential $U_\mu(r)$ was obtained by performing the self-consistent calculation with eq. (3.1). Then the single-particle wave functions used to evaluate the radial overlaps $\Omega_{j,\pi}$ were obtained by solving eq. (3.1) using this average potential shape, while scaling its overall strength to reproduce the separation energy. The HF calculation was carried out using the SGII Skyrme interaction of Sagawa and van Giai [17,18]. For the purpose of comparison, the calculation was also performed with the usual method of using a Woods-Saxon (WS) plus Coulomb single-particle potential [20].

The separation energies used to scale the average central potential were determined from experimental ground-state masses [21] and excitation energies [22]. Where experimental excitation energies were not available excitation energies found with the USD hamiltonian were used. The spectroscopic amplitudes $S(j,\Gamma\pi)$ were also evaluated using the sd-shell wave functions.

The quantities δ_{RO} obtained from the HF and WS calculations are presented in table 1. Values of δ_{RO} obtained from the HF wave functions are systematically reduced relative to the WS calculation. This reduction is due to the effects of both the Coulomb and nuclear potentials used in each calculation. The Coulomb

TABLE 1

Values for the radial-overlap correction δ_{RO} obtained with the Woods-Saxon (WS) potential and the Skyrme Hartree-Fock (HF) potential

Decaying nucleus	δ_{RO} [%]	
	WS	HF
^{34}Ar	0.732	0.369
^{34}Cl	0.561	0.438
^{30}S	1.058	0.590
^{26}Si	0.486	0.149
^{26}Al	0.229	0.205
^{22}Mg	0.425	0.191

potential of the WS procedure was that of a uniformly charged sphere containing $Z-1$ protons, whose radius was chosen to reproduce the experimental rms charge radii, with no exchange term. The WS isovector potential is generally assumed to be proportional to $N-Z$, whereas the isovector interaction in the HF procedure arises from the difference in the neutron and proton densities, leading to an isovector potential even for $N = Z$ nuclei.

To understand the difference between the proton and neutron wave functions generated with the WS and HF procedures we consider protons perturbatively relative to neutrons in ^{34}Cl. The perturbing hamiltonian in the WS procedure, δH_{WS}, is simply $V_{Coul}^{(WS)}(r)$, while in the HF procedure we have

$$\delta H_{HF} = \frac{m}{m^*(r)}\left[U_p(r) - U_n(r)\right] + V_{Coul}^{(HF)}(r),$$

where we have neglected the effects of the small isovector spin-orbit term. Plotted in fig. 1 are the quantities

$$\begin{aligned} \delta H_{Coul} &= V_{Coul}^{(HF)}(r) - V_{Coul}^{(WS)}(r), \\ \delta H_{isov} &= \frac{m}{m^*(r)}\left[U_p(r) - U_n(r)\right], \\ \delta H &= \delta H_{Coul} + \delta H_{isov}. \end{aligned} \tag{3.2}$$

δH is then the extra potential exerted on protons in the HF procedure relative to WS. In Hartree-Fock calculations protons are effectively in a potential well which is both deeper at the origin and has a higher barrier at the nuclear surface relative to neutrons. The effect on δ_{RO} due to these perturbing potentials can be seen in fig. 2 where the difference, $\delta\psi = r|\psi_n - \psi_p|$, is plotted for $0d_{\frac{3}{2}}$ radial wave functions obtained from both the WS and HF calculations. This additional potential tends to

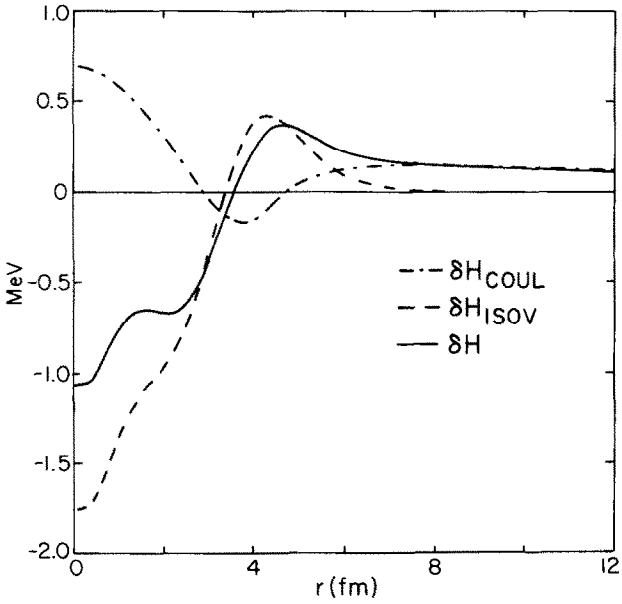

Fig. 1. Plot of the perturbing hamiltonians δH_{Coul}, δH_{isov}, and δH, defined in eq. (3.2), as a function of r.

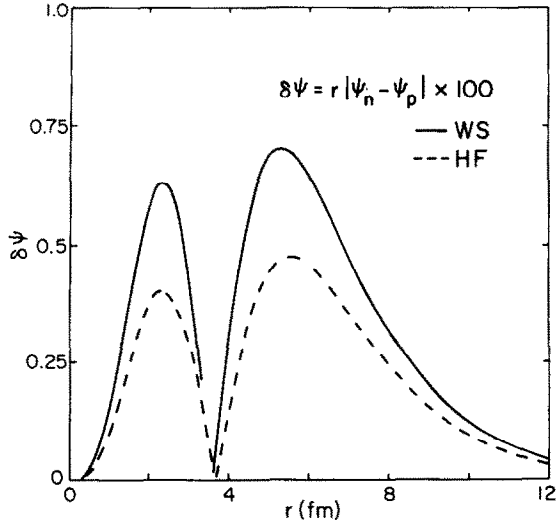

Fig. 2. Plot of the difference $\delta\psi = r|\psi_n - \psi_p| \times 100$ for the Hartree-Fock (HF) and Woods-Saxon (WS) wave functions.

draw in the proton radial wave functions relative to the neutrons, and thus reduce the value of δ_{RO}.

4. Isospin-mixing contribution to δ_C

4.1. INTRODUCTION

The contribution of δ_C due to isospin mixing, δ_{IM}, can be calculated with two equivalent methods. The first is to obtain nuclear wave functions from the shell model by adding the isospin-nonconserving (INC) interaction directly into the matrix diagonalization procedure. The Fermi matrix element correction δ_{IM} can then be calculated by simply calculating the OBTD matrix of eq. (2.4). The second method is to consider the effects of the INC potential perturbatively. The Fermi matrix element is then calculated with wave functions corrected to first order, and δ_{IM} becomes a sum of terms which are dependent on the matrix element of the INC potential between the ground state and all other states.

Since the perturbation is small the two methods are equivalent; however, each of the methods have particular advantages and disadvantages. The primary advantage of the perturbative approach is that it is easier to determine the contribution to δ_{IM} due to either specific nuclear states, or particular parts of the interaction, such as that due to the single-particle energies, the two-body matrix elements, or the tensor components of the interaction. A further advantage is that it is more straightforward to understand the relationship between the coefficients of the isobaric mass formula (IMME) and isospin-mixing amplitudes obtained from perturbation theory. The disadvantage of the perturbative method is that it involves a sum over many matrix elements connecting to a large number of exited states. In addition, the perturbative method requires the calculation of the two-body transition densities (see below) which is often time consuming. The diagonalization procedure has the advantage that the sum over the matrix elements performed in the perturbative method is done automatically during the diagonalization of the hamiltonian.

In the present work, we have used both methods. First, wave functions with good isospin were used to calculate the b- and c-coefficients of the isobaric mass formula via perturbation theory. The perturbative interaction considered is the Coulomb potential plus a phenomenological short-ranged INC potential. By allowing parameters of this potential to vary, experimental b- and c-coefficients are fit upon to obtain an empirical INC interaction. After the potential is determined, it is then added to the input hamiltonian of the shell model in the proton-neutron formalism. The isospin mixed nuclear wave functions are then obtained, and the Fermi matrix elements are calculated with these new wave functions using eq. (2.4).

4.2. $\delta_{\rm IM}$ AND THE COEFFICIENTS OF THE ISOBARIC MASS FORMULA

To understand the connection between the coefficients of the isobaric mass formula and $\delta_{\rm IM}$, we start with a calculation of $\delta_{\rm IM}$ with perturbation theory. Basis wave functions $\Psi(\Gamma, T, T_z)$ are obtained from the standard shell-model procedure and have definite angular momentum J, isospin T, and isospin projection T_z. Following the method of Blin-Stoyle [3]) and Towner and Hardy [6]), the first-order wave function of the state Γ in the presence of an isospin-nonconserving potential $V_{\rm INC}$ is given by

$$\Psi(\Gamma, T_z) = N(\Gamma, T, T_z)\psi(\Gamma, T, T_z) + \sum_{\nu} \sum_{t=|T_z|}^{T+2} a(\nu, t, T_z)\psi(\nu, t, T_z), \tag{4.2.1}$$

where the sum over ν represents the sum over all quantum numbers other than isospin, the coefficients $a(\nu, t, T_z)$ are given by

$$a(\nu, t, T_z) = \frac{\langle \psi(\nu, t, T_z)|V_{\rm INC}|\psi(\Gamma, T, T_z\rangle}{E(\nu, t) - E(\Gamma, T)}, \tag{4.2.2}$$

and the normalizing constant $N(\Gamma, T, T_z)$ satisfies the constraint

$$\{N(\Gamma, T, T_z)\}^2 + \sum_{\nu} \sum_{t=|T_z|}^{T+2} \{a(\nu, t, T_z)\}^2 = 1. \tag{4.2.3}$$

To calculate the effect of isospin mixing on Fermi β-decay, we square the matrix element of the τ_- operator between the state $\Psi(\Gamma, T_z)$ and its analogue $\Psi(\Gamma, T_z - 1)$, corrected to first order with eq. (4.2.1), to obtain

$$\begin{aligned} |M_{\rm F}|^2 &= |\langle \Psi(\Gamma, T_z - 1)|\tau_-|\Psi(\Gamma, T_z)\rangle|^2 \\ &= [T(T+1) - T_z(T_z-1)] \Bigg\{ N(\Gamma, T, T_z)N(\Gamma, T, T_z - 1) \\ &\quad + \sum_{\nu} \sum_{t=|T_z|}^{T+2} \left(\frac{t(t+1) - T_z(T_z-1)}{T(T+1) - T_z(T_z-1)} \right)^{\frac{1}{2}} a(\nu, t, T_z)a(\nu, t, T_z - 1) \Bigg\}^2 . \end{aligned} \tag{4.2.4}$$

Expanding eq. (4.2.4) and keeping terms only up to second order in $a(\nu, t, T_z)$ we find

$$\begin{aligned} |M_{\rm F}|^2 &= [T(T+1) - T_z(T_z-1)] \Bigg\{ N^2(\Gamma, T, T_z)N^2(\Gamma, T, T_z - 1) \\ &\quad + 2N(\Gamma, T, T_z)N(\Gamma, T, T_z - 1) \\ &\quad \times \sum_{\nu} \sum_{t=|T_z|}^{T+2} \left(\frac{t(t+1) - T_z(T_z-1)}{T(T+1) - T_z(T_z-1)} \right)^{\frac{1}{2}} a(\nu, t, T_z)a(\nu, t, T_z - 1) \Bigg\}. \end{aligned} \tag{4.2.5}$$

By inserting eq. (4.2.3) into eq. (4.2.5) we find

$$\delta_{\mathrm{IM}}(T_z) = \sum_{v}\Bigg[\sum_{t=|T_z|}^{T+2}\{a(v,t,T_z)\}^2 + \sum_{t=|T_z-1|}^{T+2}\{a(v,t,T_z-1)\}^2 - 2\sum_{t=|T_z|}^{T+2}\left(\frac{t(t+1)-T_z(T_z-1)}{T(T+1)-T_z(T_z-1)}\right)^{\frac{1}{2}} a(v,t,T_z)a(v,t,T_z-1)\Bigg]. \tag{4.2.6a}$$

Similarly, it can be shown that $|M_{\mathrm{F}}|^2$ for the forbidden (off-diagonal) β-decay of the state $\Psi(\Gamma, T_z)$ to $\Psi(\Gamma', T_z-1)$ is given by

$$|M_{\mathrm{F}}|^2 = [T(T+1)-T_z(T_Z-1)]\{a(\Gamma,T,T_z-1)+a(\Gamma',T,T_z)\}^2. \tag{4.2.6b}$$

A tensor decomposition of V_{INC} can be made,

$$V_{\mathrm{INC}} = \sum_{k} V_{\mathrm{INC}}^{(k)},$$

and using the Wigner-Eckart theorem the matrix elements in eq. (4.2.2) can be written as

$$\langle\Psi(v,t,T_z)|V_{\mathrm{INC}}|\Psi(\Gamma,T,T_z)\rangle = \frac{1}{(2J+1)^{\frac{1}{2}}}\sum_{k=0}^{2}(-1)^{t-T_z}\begin{pmatrix} T & k & T \\ -T_z & 0 & T_z\end{pmatrix}\langle\psi(v,t)|||V_{\mathrm{INC}}^{(k)}|||\psi(\Gamma,T)\rangle, \tag{4.2.7}$$

where the three bars in the reduced matrix element denotes a reduction in both angular momentum and isospin space. Within the framework of the shell model, the reduced matrix elements in eq. (4.2.7) can be written as a sum dependent on the single-particle and two-body matrix elements weighted respectively by the one-body and two-body transition density matrices. The reduced matrix elements then become

$$\begin{aligned}\langle\psi(v,t)|||V_{\mathrm{INC}}^{(k)}|||\psi(\Gamma,T)\rangle &= \sum_{\text{orbits}}\mathrm{OBTD}(\rho,\rho';k)\langle\mathrm{core},\rho|||V_{\mathrm{INC}}^{(k)}|||\mathrm{core},\rho'\rangle \\ &\quad+\sum_{\text{orbits}}\mathrm{TBTD}(\rho_1\rho_2;\lambda_{12}:\rho_3\rho_4;\lambda_{34};k) \\ &\quad\times\langle\rho_1\rho_2;\lambda_{12}|||V_{\mathrm{INC}}^{(k)}|||\rho_3\rho_4;\lambda_{34}\rangle,\end{aligned} \tag{4.2.8}$$

where the ket $|\mathrm{core},\rho\rangle$ represents the single nucleon in the ρth orbit outside a closed core, and the ket $|\rho\rho';\lambda\rangle$ represents the antisymmetric two-nucleon wave

function with particles in the orbits ρ and ρ' coupled to the intermediate state λ. The labels ρ and λ contain both the available angular momentum and isospin-coupling quantum numbers. The general form of the OBTD and TBTD matrices are given by [19])

$$\mathrm{OBTD}_\Gamma(\rho,\rho';\lambda) = \frac{1}{(2\lambda+1)^{\frac{1}{2}}}\langle\psi(v,t)|||[a_\rho^\dagger \times \tilde{a}_{\rho'}]^\lambda|||\psi(\Gamma,T)\rangle, \tag{4.2.9a}$$

$$\mathrm{TBTD}_\Gamma(\rho_1\rho_2;\lambda_{12}:\rho_3\rho_4;\lambda_{34}:\lambda) = -\frac{1}{[(2\lambda+1)(1+\delta_{\rho_1\rho_2})(1+\delta_{\rho_3\rho_4})]^{\frac{1}{2}}}$$

$$\times\langle\psi(v,t)|||[(a_{\rho_1}^\dagger \times a_{\rho_2}^\dagger)^{\lambda_{12}} \times (\tilde{a}_{\rho_3} \times \tilde{a}_{\rho_4})^{\lambda_{34}}]^\lambda|||\psi(\Gamma,T)\rangle, \tag{4.2.9b}$$

where $(2\lambda+1)^{\frac{1}{2}}$ is shorthand for $[(2J+1)(2T+1)]^{\frac{1}{2}}$. The intermediate couplings λ_{12} and λ_{34} are restricted by the requirement that the final coupling λ must be to an angular momentum state with $\Delta J = 0$ and isospin $\Delta T = \mathrm{k}$.

To deduce the relationship between the coefficients of the isobaric mass formula and the reduced matrix elements of eq. (4.2.9) we consider the diagonal matrix element of the interaction:

$$\langle\Psi(J,T,T_z)|V_{\mathrm{INC}}|\Psi(J,T,T_z)\rangle = E(J,T,T_z). \tag{4.2.10}$$

By applying the tensor decomposition to the potential V_{INC}, using the Wigner-Eckart theorem, and substituting for the values of the 3-j coefficients we obtain

$$E(J,T,T_z) = E^{(0)}(J,T) + T_z E^{(1)}(J,T) + [3T_z^2 - T(T+1)]E^{(2)}(J,T), \tag{4.2.11}$$

where

$$E^{(0)}(J,T) = \frac{1}{[(2J+1)(2T+1)]^{\frac{1}{2}}}\langle\Psi(J,T)|||V_{\mathrm{INC}}^{(0)}|||\Psi(J,T)\rangle,$$

$$E^{(1)}(J,T) = \frac{1}{[(2J+1)T(2T+1)(T+1)]^{\frac{1}{2}}}\langle\Psi(J,T)|||V_{\mathrm{INC}}^{(1)}|||\Psi(J,T)\rangle,$$

$$E^{(2)}(J,T) = \frac{1}{[(2J+1)(2T-1)(2T+1)(T+1)(2T+3)]^{\frac{1}{2}}}$$

$$\times\langle\Psi(J,T)|||V_{\mathrm{INC}}^{(2)}|||\Psi(J,T)\rangle. \tag{4.2.12}$$

Eq. (4.2.11) has the same form as the isobaric mass formula, i.e.

$$E(J,T,T_z) = a(J,T) + b(J,T)T_z + c(J,T)T_z^2 \tag{4.2.13}$$

with

$$a(J,T) = E^{(0)}(J,T) - T(T+1)E^{(2)}(J,T),$$
$$b(J,T) = E^{(1)}(J,T),$$
$$c(J,T) = 3E^{(2)}(J,T).$$

Again the many-body reduced matrix elements in eq. (4.2.12) can be related to the single-particle and two-body matrix elements in the same manner as in eq. (4.2.8). Therefore, the requirement that these single-particle and two-body matrix elements reproduce an experimental set of b- and c-coefficients should lead to a reliable evaluation of δ_{IM}.

4.3. DETERMINATION OF THE INC INTERACTION

Basis wave functions used as a starting point in eq. (4.2.10) were obtained from the Oxford–Buenos Aires shell-model code[23]) with the USD hamiltonian of Wildenthal[13]). The perturbing potential was taken to be of the form

$$V_{\mathrm{INC}}^{(k)} = [C^{(k)}V_{\mathrm{C}}(r) + P^{(k)}V_{\pi}(r) + R^{(k)}V_{\rho}(r)]I^{(k)}, \tag{4.3.1}$$

where $V_{\mathrm{C}}(r)$ is the Coulomb potential, $e^2/r \cdot V_{\pi}(r)$ and $V_{\rho}(r)$ are Yukawa potentials of the form

$$V_{\mu}(r) = \frac{\mathrm{e}^{-\mu r}}{\mu r},$$

with $\mu_{\pi} = 0.7\,\mathrm{fm}^{-1}$ and $\mu_{\rho} = 3.9\,\mathrm{fm}^{-1}$. The strength of each interaction in eq. (4.3.1) is embodied in the coefficients $C^{(k)}$, $P^{(k)}$, and $R^{(k)}$ which are assumed to depend only on the isospin tensor rank k. $I^{(k)}$ is an isospin operator whose form permits the INC interaction components $V_{\mathrm{INC}}^{(k)}$ to correspond to the $T = 1$ part of the proton-proton (v_{pp}), neutron-neutron (v_{nn}) and proton-neutron (v_{pn}) interactions by

$$V_{\mathrm{INC}}^{(0)} = \tfrac{1}{3}(v_{\mathrm{pp}} + v_{\mathrm{nn}} + v_{\mathrm{pn}}),$$
$$V_{\mathrm{INC}}^{(1)} = v_{\mathrm{pp}} - v_{\mathrm{nn}},$$
$$V_{\mathrm{INC}}^{(2)} = v_{\mathrm{pp}} + v_{\mathrm{nn}} - 2v_{\mathrm{pn}}. \tag{4.3.2}$$

Two-body matrix elements of eq. (4.3.1) were calculated with harmonic-oscillator wave functions with an oscillator parameter appropriate for $A = 39$, given by

$$\hbar\omega(A) = 45A^{-\frac{1}{3}} - 25A^{-\frac{2}{3}}\ \mathrm{MeV}. \tag{4.3.3a}$$

Matrix elements for a nucleus of mass A were evaluated by scaling the single-particle and two-body matrix elements of $A = 39$ by the scaling factor

$$\mathrm{SF}(A) = (\hbar\omega(A)/\hbar\omega(39))^{\frac{1}{2}}. \tag{4.3.3b}$$

Using eqs. (4.2.8) and (4.2.12), the b- and c-coefficients of the IMME can be written as a sum of parts depending on the isovector single-particle energies $\varepsilon^{(1)}(\mathrm{s}_{\frac{1}{2}})$, $\varepsilon^{(1)}(\mathrm{d}_{\frac{3}{2}})$, and $\varepsilon^{(1)}(\mathrm{d}_{\frac{5}{2}})$ (i.e. the difference between the proton and neutron single-particle energies) and the two-body matrix elements calculated with the potential of eq. (4.3.1). Hence the b- and c-coefficients of the ith state in a nucleus of mass A can be written as

$$\begin{aligned} b(i, A) = {} & \varepsilon^{(1)}(\mathrm{d}_{\frac{5}{2}})\mathrm{SP}^{(1)}(i, A, \mathrm{d}_{\frac{5}{2}}) + \varepsilon^{(1)}(\mathrm{S}_{\frac{1}{2}})\mathrm{SP}^{(1)}(i, A, \mathrm{s}_{\frac{1}{2}}) \\ & + \varepsilon^{(1)}(\mathrm{d}_{\frac{3}{2}})\mathrm{SP}^{(1)}(i, A, \mathrm{d}_{\frac{3}{2}}) + C^{(1)}\gamma^{(1)}(i, A, V_{\mathrm{C}}) + P^{(1)}\gamma^{(1)}(i, A, V_{\pi}) \\ & + R^{(1)}\gamma^{(1)}(i, A, V_{\rho}), \end{aligned} \tag{4.3.4a}$$

$$c(i, A) = C^{(2)}\gamma^{(2)}(i, A, V_{\mathrm{C}}) + P^{(2)}\gamma^{(2)}(i, A, V_{\pi}) + R^{(2)}\gamma^{(2)}(i, A, V_{\rho}), \tag{4.3.4b}$$

where the quantities $\mathrm{SP}^{(1)}(i, A, \rho)$ and $\gamma^{(k)}(i, A, V_{\mu})$ are given by

$$\mathrm{SP}^{(1)}(i, A, \rho) = \frac{\mathrm{SF}(A)}{[(2J_i+1)T_i(2T_i+1)(T_i+1)]^{\frac{1}{2}}}\,\mathrm{OBTD}_{A,i}(\rho, \rho; 1), \tag{4.3.5a}$$

$$\begin{aligned} \gamma^{(1)}(i, A, V_{\mu}) = {} & \frac{\mathrm{SF}(A)}{[(2J_i+1)T_i(2T_i+1)(T_i+1)]^{\frac{1}{2}}} \\ & \times \sum_{\text{orbits}} \mathrm{TBTD}_{A,i}(j_1 j_2; J, T = 1 : j_3 j_4; J, T = 1; \Delta J = 0, k = 1) \\ & \times \langle j_1 j_2; J, T = 1 \| V_{\mu} I^{(1)} \| j_3 j_4; J, T = 1 \rangle_{A=39}, \end{aligned} \tag{4.3.5b}$$

$$\begin{aligned} \gamma^{(2)}(i, A, V_{\mu}) = {} & \frac{\mathrm{SF}(A)}{[(2J_i+1)(2T_i-1)(2T_i+1)(T_i+1)(2T_i+3)]^{\frac{1}{2}}} \\ & \times \sum_{\text{orbits}} \mathrm{TBTD}_{A,i}(j_1 j_2; j, T = 1 : j_3 j_4; j, T = 1; \Delta J = 0, k = 2) \\ & \times \langle j_1 j_2; J, T = 1 \| V_{\mu} I^{(2)} \| j_3 j_4; J, T = 1 \rangle_{A=39}. \end{aligned} \tag{4.3.5c}$$

The reduced two-body matrix elements in eq. (4.3.5) are given by

$$\langle j_1 j_2; J, T = 1 \| V_{\mu} I^{(1)} \| j_3 j_4; J, T = 1 \rangle = [\tfrac{3}{2}(2J+1)]^{\frac{1}{2}} \times \langle j_1 j_2; J | V_{\mu} | j_3 j_4; J \rangle,$$

$$\langle j_1 j_2; J, T = 1 \| V_{\mu} I^{(2)} \| j_3 j_4; J, T = 1 \rangle = [\tfrac{5}{6}(2J+1)]^{\frac{1}{2}} \times \langle j_1 j_2; J | V_{\mu} | j_3 j_4; J \rangle.$$

The single-particle energies and the parameters $C^{(k)}$, $P^{(k)}$ and $R^{(k)}$ are then determined by performing a least-squares fit to a set of experimental b- and c-coefficients.

In the present work, 27 b- and 17 c-coefficients were used to fix the parameters of eq. (4.3.1). The b- and c-coefficients were determined from the ground-state properties given in the mass table of ref.[21]), and with the excitation energies tabulated in ref.[22]). It was computationally feasible to calculate the TBTD for the $(sd)^{\pm n}$ configurations for $n \leqq 6$. (Some model-space truncations were necessary to calculate TBTD matricies for $n = 6$. However, the difference between the isobaric mass shift calculated with these TBTD and the shift obtained with the full space proton-neutron calculation was small.) The $A = 17$–21 mass region was not considered because our harmonic-oscillator assumption for the mass dependence of the single-particle energies is more appropriate for the deeply bound "hole" states in the upper sd shell than for the loosely bound "particle" states in the lower part of the shell. However, since we wish to calculate corrections to Fermi decays for ^{22}Mg (and eventually the remaining sd-shell superallowed transitions), we needed to consider at least one mass value for $A < 28$ in order to fix the $d_{\frac{5}{2}}$ single-particle matrix element, and we have included the mass shifts of $A = 22$ nuclei in the least-squares fit.

The fitted parameters for both the b- and c-coefficients are presented in tables 2 and 3, along with the rms deviation and parameter uncertainties for each fit. It was found that an optimal fit for the b-coefficients was obtained by varying the three isovector single-particle matrix elements while restricting $C^{(1)}$ to unity and the parameters $P^{(1)}$ and $R^{(1)}$ to zero. Subsequent variations of these parameters did not lead to a significant reduction in either the rms deviation or the parameter uncertainties. Hence, the isovector interaction used in this work was determined by varying only the isovector single-particle energies, and was evaluated with the parameters given in the first row of table 2.

TABLE 2

Single-particle energies and potential strength parameters obtained from fits to b-coefficients

$\varepsilon^{(1)}(d_{5/2})$	$\varepsilon^{(1)}(s_{1/2})$	$\varepsilon^{(1)}(d_{3/2})$	$C^{(1)}$	$P^{(1)}$ [MeV]	$R^{(1)}$ [MeV]	rms [keV]
3.325(15)	3.304(16)	3.346(7)	1.00	0.0	0	26.5
3.348(74)	3.445(18)	3.484(12)	0.96(2)	0.0	0	25.0
3.342(80)	3.426(18)	3.468(15)	0.94(4)	0.2(4)	0	24.8
3.347(88)	3.451(18)	3.498(15)	1.08(2)	−1.5(3)	76(120)	24.9
3.342(78)	3.427(18)	3.470(15)	0.96(2)	0.0	11(18)	24.8
3.348(81)	3.418(18)	3.454(15)	1.00	−0.2(2)	0	25.8
3.345(81)	3.438(18)	3.482(15)	1.00	−0.5(3)	34(23)	24.8
3.323(43)	3.294(17)	3.337(17)	1.00	0.0	4(18)	26.5

Single-particle energies are given in MeV, while potential strengths are defined in eq. (4.3.1) of the text. Uncertainties for each parameter are given in parentheses. Parameters with no uncertainty were not varied. The isovector part of the INC interaction was evaluated using the parameters in the first row.

TABLE 3

Fitted parameters obtained from fits to c-coefficients

$C^{(2)}$	$P^{(2)}$ [MeV]	$R^{(2)}$ [MeV]	rms [keV]
1.00	0.0	0	35.0
1.17(2)	0.0	0	20.1
0.82(4)	2.0(2)	0	8.2
0.99(2)	0.0	81(9)	8.1
0.93(19)	0.7(20)	53(87)	8.1
1.00	1.05(8)	0	12.8
1.00	0.0	78(4)	8.2
1.00	0.1(3)	83(18)	8.1

Strengths are defined in eq. (4.3.1) of the text. Uncertainties for each parameter are given in parentheses. Parameters with no uncertainty were not varied. The isotensor part of the INC interaction was evaluated using the parameters in the seventh row.

It is interesting to compare the fitted isovector single-particle energies extrapolated to $A = 17$ with eq. (4.3.3b), $\varepsilon^{(1)}_{\rm fit}(d_{\frac{5}{2}}) = 3.697$ MeV, $\varepsilon^{(1)}_{\rm fit}(s_{\frac{1}{2}}) = 3.674$ MeV and $\varepsilon^{(1)}_{\rm fit}(d_{\frac{3}{2}}) = 3.721$ MeV, with the experimental values determined from ^{17}F and ^{17}O [refs. [21,22]], $\varepsilon^{(1)}_{\rm exp}(d_{\frac{5}{2}}) = 3.543$ MeV, $\varepsilon^{(1)}_{\rm exp}(s_{\frac{1}{2}}) = 3.168$ MeV and $\varepsilon^{(1)}_{\rm exp}(d_{\frac{3}{2}}) = 3.561$ MeV. The fact that the experimental $A = 17$ values are smaller than those needed for the upper sd shell is a consequence of the fact that these levels are loosely bound relative to ^{16}O (unbound in the case of the $d_{\frac{3}{2}}$ level in ^{17}F), and, hence, have a larger rms radius and smaller Coulomb energy. This effect is particularly large for the $s_{\frac{1}{2}}$ orbit because of the absence of a centifugal barrier.

In order to minimize the rms deviation in the fit to the c-coefficients an additional short-range potential was necessary (see table 3). An optimal fit was obtained by fixing $C^{(2)}$ to unity, $P^{(2)}$ to zero and then varying $R^{(2)}$. The parameters used to determine the isotensor interaction are listed in the seventh row of table 3.

The values of the b- and c-coefficients obtained with these isovector and isotensor interactions are presented in tables 4 and 5, and are shown graphically in figs. 3 and 4.

4.4. RESULTS FOR $\delta_{\rm IM}$

The isopin-mixing corrections to the Femi matrix elements for ^{22}Mg, ^{34}Cl, and ^{34}Ar were evaluated using eq. (2.10b) and are presented in table 6. The quantity $\beta(j_{\rm n}, j_{\rm p}; 0)$ was evaluated with isospin-mixed wave functions obtained by adding the fitted INC interactions found in subsect 4.3 to the USD hamiltonian. To include the INC interaction the matrix elements of the USD hamiltonian were assumed to represent the average (isoscalar) nucleon-nucleon interaction. The

TABLE 4

Comparison of fitted b-coefficients with experimental values

A	J	T	b (exp) [MeV]	b (fit) [MeV]
22	0	1	4.597(2)	4.593
	2	1	4.583(2)	4.586
	4	1	4.573(10)	4.587
	2	1	4.571(10)	4.584
34	0	1	6.559(1)	6.546
	2	1	6.541(1)	6.525
	2	1	6.551(2)	6.533
	0	1	6.537(2)	6.521
35	$\frac{3}{2}$	$\frac{1}{2}$	6.747(2)	6.736
	$\frac{1}{2}$	$\frac{1}{2}$	6.712(2)	6.677
	$\frac{5}{2}$	$\frac{1}{2}$	6.734(2)	6.716
	$\frac{3}{2}$	$\frac{1}{2}$	6.654(2)	6.673
	$\frac{5}{2}$	$\frac{1}{2}$	6.727(3)	6.659
	$\frac{1}{2}$	$\frac{1}{2}$	6.664(2)	6.661
	$\frac{3}{2}$	$\frac{3}{2}$	6.666(10)	6.673
36	2	1	6.830(4)	6.832
	3	1	6.836(7)	6.833
	1	1	6.806(7)	6.821
	0	2	6.827(13)	6.837
37	$\frac{3}{2}$	$\frac{1}{2}$	6.931(1)	6.924
	$\frac{1}{2}$	$\frac{1}{2}$	6.890(10)	6.929
	$\frac{5}{2}$	$\frac{1}{2}$	6.884(10)	6.966
	$\frac{3}{2}$	$\frac{3}{2}$	6.983(10)	6.997
	$\frac{1}{2}$	$\frac{3}{2}$	6.947(12)	6.969
38	0	1	7.109(5)	7.116
	2	1	7.129(6)	7.159
39	$\frac{3}{2}$	$\frac{1}{2}$	7.313(4)	7.317
	$\frac{1}{2}$	$\frac{1}{2}$	7.257(4)	7.292

$T = 1$ part of nucleon-nucleon matrix elements are then

$$v_{pp} = V^{(0)} + \tfrac{1}{2}V^{(1)}_{INC} + \tfrac{1}{6}V^{(2)}_{INC},$$

$$v_{nn} = V^{(0)} - \tfrac{1}{2}V^{(1)}_{INC} + \tfrac{1}{6}V^{(2)}_{INC},$$

$$v_{pn} = V^{(0)} - \tfrac{1}{3}V^{(2)}_{INC},$$

TABLE 5

Comparison of fitted c-coefficients with experimental values

A	J	T	c (exp) [keV]	c (fit) [keV]
22	0	1	316(2)	315
	2	1	282(2)	272
	4	1	235(10)	226
	2	1	231(10)	228
34	0	1	284(2)	282
	2	1	235(2)	228
	2	1	196(2)	197
	0	1	235(2)	252
35	$\frac{3}{2}$	$\frac{3}{2}$	214(10)	204
36	2	1	146(4)	145
	3	1	214(7)	229
	1	1	188(7)	199
	0	2	201(13)	204
37	$\frac{3}{2}$	$\frac{3}{2}$	196(10)	204
	$\frac{1}{2}$	$\frac{3}{2}$	210(14)	218
38	0	1	285(5)	282
	2	1	199(6)	198

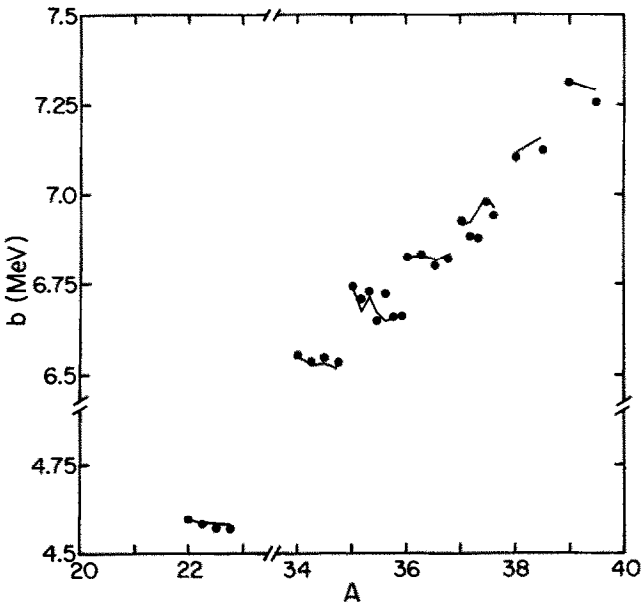

Fig. 3. Plot of b-coefficients. Experimental data are represented by circles, while the line passes through the fitted values. The coefficients are plotted in the same order as they appear in table 4.

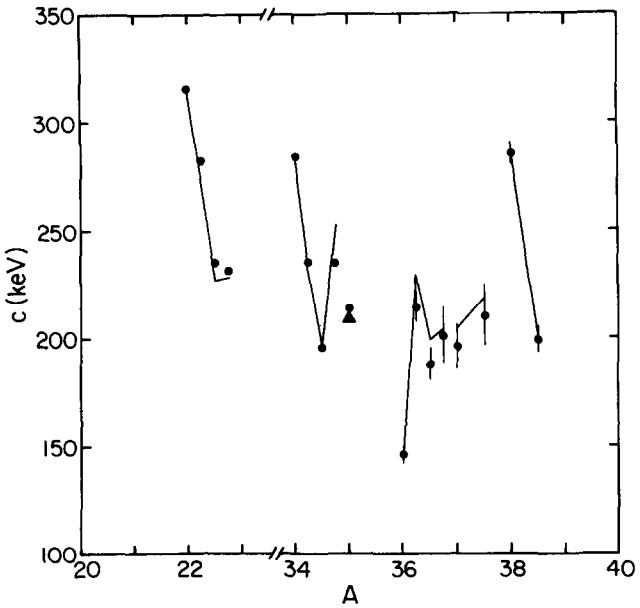

Fig. 4. Plot of c-coefficients. Experimental data are represented by circles, while the line passes through the fitted values and the triangle represents the fitted value for $A = 35$. The coefficients are plotted in the same order as they appear in table 5.

with

$$V^{(0)} = V_{\mathrm{USD}} + \tfrac{1}{3} V_{\mathrm{Coul}}$$

where V_{USD} are the sd-shell hamiltonian matrix elements of ref. [13]), and $V_{\mathrm{INC}}^{(k)}$ are the total fitted two-body matrix elements obtained for the isovector ($k = 1$) and the isotensor ($k = 2$) parts of the INC interaction. Note that the presence of $\frac{1}{3}$ the Coulomb potential in the neutron-neutron and proton-neutron interactions is cancelled by the Coulomb part of the isovector and/or isotensor interactions.

Values of δ_{IM} for ^{30}S, ^{26}Si, and ^{26}Al were not evaluated because of the computational restrictions that arise while attempting to use the full or nearly full

TABLE 6

Values for the isospin-mixing correction δ_{IM}

Decaying nucleus	δ_{IM} [%]
^{34}Ar	0.006
^{34}Cl	0.056
^{22}Mg	0.018

configuration space when calculating properties of nuclei in the middle of the sd shell. Currently, an optimization of the computer codes is in progress, and it is hoped that the values for these remaining sd-shell transitions can be calculated in the future.

5. Isospin-forbidden β-decay

In this section results for the Fermi matrix element between the lowest 0^+, $T = 1$ state and the first excited 0^+, $T = 1$ state for the decays of ^{34}Cl and ^{34}Ar are discussed. The Fermi matrix element for these forbidden transitions can be evaluted using eq. (2.8), except that the sum over $\mathrm{OBTD}^{\mathrm{T}}(j_{\mathrm{n}}, j_{\mathrm{p}}; 0)$ is zero. Hence, M_{F} differs from zero only if the radial integrals $\Omega_{j,\pi}$ differ from unity, or if there is mixing due to the INC interaction between these two states. These two contributions to M_{F} for ^{34}Ar and ^{34}Cl were evaluated in the same manner as the correction δ_{C}, and are presented in table 7. With these values for the Fermi matrix element, the strength of the isospin forbidden β-decay of ^{34}Ar and ^{34}Cl is supressed relative to the superallowed transitions by 2.3×10^{-8} and 3.6×10^{-4}, respectively. Although there are as yet no experimental values with which to compare, it is interesting to note that the suppression of 6.9×10^{-4} found in ref. [24]) for the decay of $^{+2}$Sc is close to the value we calculate for ^{34}Cl.

TABLE 7

Values of the Fermi matrix element for the isospin-forbidden β-decay of the lowest 0^+, $T = 1$ state to the first excited 0^+, $T = 1$ state for ^{34}Ar and ^{34}Cl from the radial overlap (RO) and from the isospin-mixing (IM) term

Decaying nucleus	M_{F}		$\lvert M_{\mathrm{F}}\rvert^2$
	RO	IM	RO+IM
^{34}Ar	1.8×10^{-4}	-3.5×10^{-5}	4.6×10^{-8}
^{34}Cl	1.3×10^{-4}	-2.7×10^{-2}	7.2×10^{-4}

6. Discussion

In table 8 we present a comparison of the values for δ obtained in the present work and with values obtained previously[6-8]). The radial-overlap corrections evaluated from the Woods-Saxon potential shown in table 1 and those found in ref. [8]) (also evaluated with a Woods-Saxon potential and eq. (2.10a)) are in general agreement. Again, we note that by including the effects of the induced isovector interaction the radial-overlap contribution to δ_{C} is reduced relative to previous estimates.

TABLE 8

Comparison of the corrections to the Fermi matrix element obtained in the present work and with the values in refs.[6,8]) (values of δ are given in %)

Decaying nucleus	Present work			Previous values[6,8])		
	δ_{IM}	δ_{RO}	δ_C	δ_{IM}	δ_{RO}	δ_C
^{34}Ar	0.006	0.369	0.375	0.13	0.91	1.04
^{34}Cl	0.056	0.438	0.494	0.23	0.62	0.85
^{30}S	[a])	0.590	–	0.34	0.87	1.21
^{26}Si	[a])	0.149	–	0.04	0.38	0.42
^{26}Si	[a])	0.205	–	0.07	0.27	0.34
^{22}Mg	0.018	0.191	0.209	0.06	0.29	0.35

[a]) Not calculated in the present work.

The discrepancy which exists between the values of δ_{IM} obtained in the present work compared to those of Towner and Hardy[6]) is due to the different zeroth-order wave functions and/or the INC interaction used. The zeroth-order wave functions used in ref.[6]) were obtained with a modified surface delta interaction (MSDI) in a truncated sd-shell model space. The truncation restriction was that no more than two holes in the $d_{\frac{5}{2}}$ orbit were allowed. The INC interaction of ref.[6]) was obtained by: (i) adding Coulomb matrix elements to the proton-proton two-body matrix elements, (ii) increasing the $T = 1$ part of the MSDI proton-neutron matrix elements by 2%, and (iii) using the $A = 17$ energy levels to determine the isovector single-particle energies (i.e. $\varepsilon^{(1)}(d_{\frac{5}{2}}) = 3.544$ MeV, $\varepsilon^{(1)}(s_{\frac{1}{2}}) = 3.168$ MeV and $\varepsilon^{(1)}(d_{\frac{3}{2}}) = 3.56$ MeV). In addition no A-dependence in the single-particle energies was assumed, and the value of $\hbar\omega$ for $A = 34$ used in ref.[6]) was 11.2 MeV, while the value of 11.5 MeV was used in the present work.

The effects of the the model-space truncation were investigated by evaluating δ_{IM} with hamiltonian of the present work in the truncated model space used in ref.[6]). The values of δ_{IM} obtained for ^{34}Ar and ^{34}Cl in the truncated model space are 0.004% and 0.048% respectively, and do not differ much from the full-space values of 0.006% and 0.056%.

In order to determine whether the starting wave functions or the INC interaction are responsible for the discrepancy in δ_{IM}, both the IMME coefficients and δ_{IM} for $A = 34$ were evaluated with all possible combinations of the isoscalar interaction, isovector single-particle energies, and the two-body INC interaction of the present work and that of ref.[6]). The results of these calculations are presented in table 9 along with the experimental IMME coefficients. The values of δ_{IM} evaluated with the USD interaction are consistently smaller in magnitude than those evaluated with the MSDI interaction, suggesting a dependence in δ_{IM} on the starting wave functions. A comparison of the lowest $T = 0$ and $T = 1$ excitation energies obtained with both the MSDI and USD interactions with experimental

TABLE 9

Comparison of IMME coefficients and δ_{IM} evaluated with the combinations of the isoscalar interaction, isovector single-particle energies, and the two-body INC interaction

Isoscalar	INC				δ_{IM} [%]	
	single-particle	two-body	b [MeV]	c [keV]	^{34}Ar	^{34}Cl
MSDI	A	A	6.594	277	0.136	0.276[a]
MSDI	A	B	6.636	293	0.135	0.276
MSDI	B	A	6.479	284	0.019	0.078
MSDI	B	B	5.521	300	0.016	0.076
USD	A	A	6.641	292	0.055	0.186
USD	A	B	6.684	285	0.052	0.178
USD	B	A	6.497	297	0.009	0.061
USD	B	B	6.548	281	0.006	0.056
experimental IMME coefficients			6.559	284		

The labels MSDI and A refer to the isoscalar and INC interactions used in ref.[6]), while the labels USD and B represent the universal sd-shell hamiltonian[13]) and fitted INC interaction of the present work.

[a]) Values obtained by Towner and Hardy[25]) for these quantities are $b = 6.596$ MeV, $c = 278$ keV, $\delta_{IM}(^{34}\text{Ar}) = 0.132\%$, and $\delta_{IM}(^{34}\text{Cl}) = 0.234\%$.

values is presented in table 10, with generally better agreement with experiment occurring with the USD excitation energies.

A further discrepancy lies in the selection of the isovector single-particle energies. From a comparison between the values of δ_{IM} obtained with the single-particle

TABLE 10

Comparison between MSDI, USD and experimental excitation energies (in MeV) for $A = 34$

J	T	exp	USD	MSDI
0	1	0.000	0.000	0.00
3	0	0.146	0.133	−0.13
1	0	0.461	0.317	−0.45
1	0	0.666	0.661	−0.19
2	0	1.230	1.142	0.39
2	0	1.887	1.712	1.43
2	1	2.127	2.200	1.99
3	0	2.181	2.032	1.19
4	0	2.376	2.394	2.07
2	1	3.303	3.138	2.68
5	0	3.646	3.762	3.59
0	1	3.914	3.905	3.32
4	0	3.964	3.897	3.20
1	1	4.074	4.302	3.87
2	1	4.114	4.896	5.09
3	1	4.876	4.773	4.18

No more than two excitation energies with a given J- and T-value are tabulated.

energies of ref.[6]) and the fitted single-particle energies of this work, it is apparent that δ_{IM} is sensitive to the single-particle energies. The isospin mixing amplitudes of eq. (4.2.6), in fact are sensitive to the relative difference in the isovector single-particle energies, $\varepsilon^{(1)}(\rho) - \varepsilon^{(1)}(d_{\frac{3}{2}})$. For $A = 34$ the relative difference in the isovector single-particle energies for the $s_{\frac{1}{2}}$ and $d_{\frac{3}{2}}$ orbits are -21 keV and 21 keV for the INC interaction of the present work, and -370 keV and 20 keV for the INC interaction of ref.[6]). It is this difference between the isovector single-particle energies of ref.[6]) and the present work that is primarily responsible for the discrepancy that exists between the values of δ_{IM}. We feel that the single-particle matrix elements determined by the fitting procedure are more appropriate for the upper sd-shell region than those derived from the mass differences in $A = 17$ analogues because of the loosely bound nature of the $A = 17$ "particle" states.

To further understand the values of δ_{IM} presented here and in ref.[6]) the perturbation expansion of eq. (4.2.6) was obtained for the $A = 34$ analogues by evaluating the direct overlap between the isospin-mixed ground-state wave functions and 16 $J^\pi = 0^+$ states of the unperturbed system, with $0 \leqq T \leqq 2$. Results of the perturbation expansion are presented in tables 11 and 12 for the interactions of ref.[6]) and the present work, respectively. From this expansion it is apparent that our fitted INC interaction predicts less mixing to excited states than

TABLE 11

Isospin-mixing amplitudes and contribution to δ_{IM} due to the 15 lowest 0^+ states ($T = 0$ and 1) and the first $T = 2$ state evaluated with the interaction in ref.[6])

Excitation energy [MeV]	T	Isospin-mixing amplitudes [$\times 10^{-4}$]			δ_{IM} [%]	
		^{34}Ar	^{34}Cl	^{34}S	^{34}Ar	^{34}Cl
3.314	1	47	291	696	0.0595	0.1640
4.924	0	0	−96	0	0.0092	0.0092
5.400	1	−310	−83	119	0.0515	0.0408
5.437	0	0	2	0	0.0000	0.0000
5.749	0	0	68	0	0.0046	0.0046
6.305	1	−125	182	−222	0.0942	0.1632
7.020	1	69	138	90	0.0048	0.0023
7.812	1	45	−31	−87	0.0058	0.0031
7.950	0	0	8	0	0.0001	0.0001
8.462	1	21	−4	103	0.0006	0.0114
8.943	1	−55	13	−53	0.0046	0.0044
8.983	0	0	−1	0	0.0000	0.0000
9.335	0	0	1	0	0.0000	0.0000
9.766	0	0	−11	0	0.0001	0.0001
9.929	1	14	−3	30	0.0003	0.0011
12.538	2	69	80	−67	−0.0080	0.0295
		total			0.2273	0.4338

Excitation energies are the unperturbed values given by the MSDI hamiltonian.

TABLE 12

Isospin-mixing amplitudes and contribution to δ_{IM} due to the 16 lowest 0^+ states evaluated with the interaction used in the present work

Excitation energy [MeV]	T	Isospin-mixing amplitudes [$\times 10^{-4}$]			δ_{IM} [%]	
		^{34}Ar	^{34}Cl	^{34}S	^{34}Ar	^{34}Cl
3.905	1	36	36	227	0.0000	0.0365
5.172	1	48	−39	−22	0.0076	0.0003
6.111	0	0	39	0	0.0015	0.0015
7.116	1	−10	−44	3	0.0012	0.0022
7.605	0	0	3	0	0.0000	0.0000
7.919	1	−5	4	5	0.0001	0.0000
8.296	0	0	−8	0	0.0001	0.0001
8.877	1	15	13	−68	0.0000	0.0066
9.881	1	−10	21	−7	0.0010	0.0008
10.400	0	0	2	0	0.0000	0.0000
11.373	1	−25	14	−44	0.0015	0.0034
11.422	1	−3	−7	−4	0.0000	0.0000
11.949	0	0	0	0	0.0000	0.0000
12.168	2	26	22	12	−0.0008	0.0015
12.495	0	0	1	0	0.0000	0.0000
12.531	1	16	−22	−16	0.0014	0.0000
		total			0.0136	0.0526

Excitation energies are the unperturbed values given by the USD hamiltonian.

does the INC interaction of ref. [6]), while both interactions predict that isospin mixing in ^{34}S is more pronounced than in either ^{34}Ar or ^{34}Cl. In the expansions of both tables the total contribution due to these 16 states deviate from the diagonalization values shown in table 8, indicating mixing to still higher states. These deviations, however, are larger for the expansion presented in table 11, and in fact the values of δ_{IM} must be reduced considerably. As can be seen from eq. (4.2.6), negative contributions to the expansion can occur only via mixing with $T = 2$ and $T = 3$ states, and, therefore, the INC interaction of ref. [6]) predicts more mixing to these higher-isospin states than does our fitted INC interaction. Finally, since the contribution to δ_{IM} due to $T = 1$ states is the square of the difference between the mixing amplitudes, the small value obtained for ^{34}Ar with the our fitted interaction is explained by the fact that the mixing amplitudes for the lowest $T = 1$ states are approximately equal in both ^{34}Ar and ^{34}Cl.

In order to understand the variations in experimentally determined ft values [12]), we hope to extend our calculations and methods to obtain values of δ_C for other transitions of interest in the 0p, 1s0d, and 1p0f shells. We also hope to test the fitted INC interaction by comparing theoretical estimates with experimental results for isospin-forbidden processes such as the forbidden Fermi β-decay of ^{24m}Al [ref. [26])], ^{24}Mg [ref. [27])], and ^{28}Mg [ref. [28])] and the isospin-forbidden proton or neutron decay of $T = \frac{3}{2}$ states in $A = 4N + 1$ nuclei [29]).

Finally, we discuss what can be learned about the vector coupling constant G_V by combining our calculated δ_C for ^{34}Cl with the experimental ft value. The vector coupling constant is extracted from eqs. (1.1) and (2.1) by inserting $f_R t = 3103.9 \pm 2.9$s [ref.[12])] and $\delta_C = 4.94 \times 10^{-3}$ (see table 8), yielding $G_V/(\hbar c)^3 = (1.14651 \pm 0.00058) \times 10^{-5}$ GeV^{-2}.

The vector coupling constant for nucleon β-decay can be related to the coupling constant for muon decay, G_μ, by

$$\frac{G_V^2}{G_\mu^2} = \cos^2\theta_C(1 + \Delta_\beta - \Delta_\mu), \tag{6.1}$$

where θ_C is the Cabibbo angle and the quantities Δ_β and Δ_μ are "inner" radiative corrections to the nucleon and muon decays. The difference $\Delta_\beta - \Delta_\mu$ is given by[30])

$$\Delta_\beta - \Delta_\mu = \frac{\alpha}{2\pi}\left[3\ln\left(\frac{M_Z}{M_p}\right) + 6\bar{Q}\ln\left(\frac{M_Z}{M_A}\right) + 2C + \ldots\right]. \tag{6.2}$$

where $3\ln(M_Z/M_p)$ is actually the difference between two terms, $3[\ln(M_W/M_p) - \ln(M_Z/M_W)]$. The first of these is due to the vector current in the local V − A theory, while the second is due to Z-boson exchange between the muon and electron in the muon decay. The remaining terms, $6\bar{Q}\ln(M_Z/M_A) + 2C$, arise from corrections to β-decay due to the axial-vector current mediated by an axial-vector boson af mass M_A. $\bar{Q}$ is the average charge of the particpating quarks (for u- and d-quarks $\bar{Q}$ is $\frac{1}{6}$). The quantity C is the least understood part of eq. (6.2), but is thought to be small relative to the remaining terms. Present estimates for C are unity[31]) and -0.5 [ref.[32])].

In order to compare the various quantities in eq. (6.1) two courses may be followed. First we can take the value of the Cabibbo angle as determined from hyperon decay and test the validity of eq. (6.2), or alternatively, assume the value of $\Delta_\beta - \Delta_\mu$ to be determined by eq. (6.2) and obtain the Cabibbo angle with eq. (6.1). Taking $G_\mu/(\hbar c)^3 = (1.166347 \pm 0.00013) \times 10^{-5}$ GeV^{-2} [refs.[33,34])], we find the ratio in eq. (6.1) to be 0.9663 ± 0.0010. Using the value of the Cabibbo angle as determined from hyperon decay, $\theta_C = 0.232 \pm 0.003$ [ref.[35])], and quantities in eq. (6.2) as $M_Z = 92.9 \pm 1.6$ GeV [refs.[36,37])], $M_A = 1.275 \pm 0.0030$ GeV [the A_1 meson mass[33])]; we determine C to be -0.7 ± 0.8. Or, following the second course and taking the conservative estimate $C = 0 \pm 1$ we find the Cabibbo angle to be 0.234 ± 0.006, in good agreement with the hyperon decay value given above.

We acknowledge many helpful discussions with Dr. Ian Towner. This research was supported in part by the National Science Foundation grant no. PHY-83-12245.

References

1) R. J. Blin-Stoyle and S. K. Nair, Nucl. Phys. **A105** (1967) 640
2) T. A. Halpern and B. Chern, Phys. Rev. **175** (1968) 1314
3) R. J. Blin-Stoyle, Isospin in nuclear physics, ed. D. H. Wilkinson (North-Holland, Amsterdam, 1969) pp. 115–172
4) J. Damgaard, Nucl. Phys. **A130** (1969) 233
5) R. J. Blin-Stoyle and J. M. Freeman, Nucl. Phys. **A150** (1970) 369
6) I. S. Towner and J. C. Hardy, Nucl. Phys. **A205** (1973) 33
7) J. C. Hardy and I. S. Towner, Nucl. Phys. **A254** (1975) 221
8) I. S. Towner, J. C. Hardy and M. Harvey, Nucl. Phys. **A284** (1977) 269
9) D. H. Wilkinson, Phys. Lett. **67B** (1977) 13
10) I. S. Towner and J. C. Hardy, Phys. Lett. **73B** (1978) 20
11) A. Sirlin, Phys. Rev. **164** (1967) 1767
12) V. T. Koslowsky, Ph. D. thesis, University of Toronto (1983)
13) B. H. Wildenthal, Progress in Particle and Nuclear Physics, ed. D. H. Wilkinson (Pergamon, Oxford, 1984) vol. II, p. 5
14) D. Vautherin and D. M. Brink, Phys. Rev. **C5** (1972) 626
15) C. B. Dover and N. V. Giai, Nucl. Phys. **A190** (1972) 373
16) M. Beiner, H. Flocard, N. V. Giai and P. Quentin, Nucl. Phys. **A238** (1975) 29
17) Nguyen Van Giai and H. Sagawa, Nucl. Phys. **A371** (1981) 1
18) Nguyen Van Giai and H. Sagawa, Phys. Lett. **106B** (1981) 379
19) P. J. Brussaard and P. W. M. Glaudemans, Shell-model applications in nuclear spectroscopy, (North-Holland, Amsterdam, 1977)
20) B. A. Brown *et al.*, Phys. Rev. **C26** (1982) 2247
21) A. H. Wapstra and K. Bos, 1982 atomic mass evaluation, Nuclear Data Center, Brookhaven National Laboratory, unpublished
22) P. M. Endt and C. van der Leun, Nucl. Phys. **A310** (1978) 1;
F. Ajzenberg-Selove, Nucl. Phys. **A375** (1982) 1
23) W. D. M. Rae, A. Etchegoyen, N. S. Godwin and B. A. Brown, OXBASH, The Oxford-Buenos Aires shell-model code, unpublished
24) A. M. Sandorfi, C. J. Lister, D. E. Alburger and E. K. Warburton, Phys. Rev. **C22** (1980) 2213
25) I. S. Towner, private communication
26) A. Ray, C. D. Hoyle and E. C. Adelberger, Nucl. Phys. **A378** (1982) 29
27) C. D. Hoyle, E. C. Adelberger, J. S. Blair, K. A. Snover, H. E. Swanson and R. D. Von Lintig, Phys. Rev. **C27** (1983) 27
28) D. E. Alburger and E. K. Warburton, Phys. Rev. **C20** (1979) 793
29) J. F. Wilkerson, R. E. Anderson, T. B. Clegg, E. J. Ludwig and W. J. Thompson, Phys. Rev. Lett. **51** (1983) 2269
30) A. Sirlin, Rev. Mod. Phys. **50** (1978) 573
31) A. Sirlin, Nucl. Phys. **B71** (1974) 29
32) E. S. Abers, D. A. Dicus, R. E. Norton and H. R. Quinn, Phys. Rev. **167** (1968) 1461
33) Review of particle properties, Rev. Mod. Phys. **56** (1984) S1
34) K. L. Giovanetti *et al.*, Phys. Rev. **D29** (1984) 343
35) M. Roos, Nucl. Phys. **B77** (1974) 420
36) G. Arnison *et al.*, Phys. Lett. **126B** (1983) 398
37) P. Bagnaia *et al.*, Phys. Lett. **129B** (1983) 130